Volume 1 | Number 1 | Jan 2013 | Pages 1–100

CrystEngComm

www.rsc.org/crystengcomm

ROYAL SOCIETY OF CHEMISTRY

ROYAL SOCIETY OF CHEMISTRY

www.rsc.org/crystengcomm

Journal Name

CrystEngComm

Dynamic Article Links ▶

ARTICLE TYPE

Enhancing Crystallization of Poly(L-lactide) by a Montmorillonitic Substrate Favoring Nucleation

Hongwei Zhao[a,b], Yijie Bian[a], Mingzhi Xu[a], Changyu Han*[a], Yi Li[a], Qinglin Dong[a], Lisong Dong[a]

Montmorillonite (MMT) generally has weak nucleating ability or even retardant crystallization for poly (L-lactide) (PLLA) depending on the dispersion morphology in matrix. A novel MMT with nucleating surface (NMMT) supported by chemically calcium phenylphosphonic acid (PPCa) (an effective nucleant for PLLA), is prepared through the chemical reaction between phenylphosphonic acid (PPOA) and 10 calcium ion on the surface of MMT for the first time. Differential scanning calorimetry, infrared spectrometry and wide-angle X-ray diffraction confirm the reaction between PPOA and the Ca-montmorillonite and formation of PPCa on the surface of MMT. Then, NMMT was introduced into PLLA via simple melt blending. The most intriguing result is that the crystallization rate of PLLA greatly increases after incorporation of NMMT, and the crystallization rate of PLLA increases with increasing 15 NMMT fraction and decreasing MMT/PPOA mass ratio. The nucleation density of PLLA increases and the spherulite size decreases significantly in the presence of NMMT. Epitaxy is the possible mechanism to explain the nucleation phenomenon of PLLA/NMMT system. Moreover, the tensile results show that NMMT has a strengthening effect on the amorphous PLLA. Through a short time annealing procedure, the mechanical properties such as tensile modulus and storage modulus of PLLA are improved by the 20 addition of NMMT.

Introduction

Poly(L-lactide) (PLLA) has attracted much attention because it is biodegradable, biocompatible, producible from renewable resources, and nontoxic to the human body and the environment. 25 Recent innovation on the production process has lowered significantly the production cost, which further stimulates the investigation on its property and potential applications. However, a serious shortcoming of PLLA is its relatively slow crystallization rate. Since PLLA is a semicrystalline polymer, 30 controlled crystallization rate and morphology are extremely important in determining its physical and chemical properties.[1-5]

Addition of nucleating agent (NA) into polymer matrix has been proved to be an effective approach to enhance the crystallization rate by lowering the surface free energy barrier 35 toward nucleation and initiating crystallization at higher temperatures upon cooling.[6-9] Tremendous efforts in the scientific community have been paid toward the improvement of PLLA crystallization rate by adding NAs.[10] Tsuji et al. found that the acceleration effects of additives on the overall 40 crystallization of PLLA decreased in the following order during cooling from the melt: poly(D-lactic acid) > talc > C60 > montmorillonite > polysaccharides.[11] Subsequently, the same research group, in another study,[12] found that biodegradable poly(glycolic acid) (PGA) could enhance the nucleation of PLLA 45 significantly. Zhou et al. found that carbonated hydroxyapatite enhanced the nucleation rate but reduced the spherulite growth

rate of PLLA.[13] Both multi-wall carbon nanotubes (MWCNTs) and polyhedral oligomeric silsesquioxanes (POSS) were reported to be efficient nucleating agents for the crystallization of PLLA, 50 and the enhancement of crystallization was dependent on the types and the contents of the nanofillers.[14,15] Fu et al. found that N, N', N"-tricyclohexyl-1,3,5-benzenetricarboxylamide was a novel nucleating agent for the crystallization of PLLA and demonstrated that the superstructure of PLLA could be controlled 55 by the nucleating agent.[16] Li and Huneault investigated the effect of talc, sodium stearate, and calcium lactate as potential nucleating agents,[17] and it was showed that the combination of NA and plasticizer was necessary to develop significant crystallinity at high cooling rates. Orotic acid is a bio-based 60 chemical that was recently investigated.[18] As little as 0.3 wt% orotic acid had a significant effect on crystallinity development in non-isothermal and isothermal mode. Moreover, stereocomplexation between PLLA and poly(D-lactic acid) (PDLA) was one of the most effective and promising methods for 65 increasing crystallization rate of poly(lactic acid) (PLA)-based materials.[19-23] It was found that the overall crystallization rate of PLA stereocomplex was much higher than that of pure PLLA or PDLA, due to extremely high radius growth rate and density (number per unit area or volume) of stereocomplex spherulites 70 and a very short induction period for the formation of stereocomplex spherulites compared to those of PLLA or PDLA spherulites. However, a high production cost of PDLA greatly limits the wide applications of the stereocomplexed PLA

materials. Besides aforementioned nucleating agents, layered metal phosphonates have exhibited a notable nucleating effect on PLA. Pan et al. compared the nucleation effect of zinc phenylphosphonate (PPZn) to that of talc and PDLA at 1% nucleating agent content.[24] In isothermal tests, PPZn was more effective than talc and PDLA in reducing the crystallization half-time, $t_{1/2}$, of PLA. In previous works, the effect of metal type on PLA/layered metal phosphonate composites was investigated by comparing zinc, calcium and barium phosphonates (PPZn, PPCa and PPBa).[25] It was found that the nucleating ability decreased in the following order PPZn > PPCa > PPBa due to the different dispersion and interfacial interaction of nucleating agents with PLA matrix. Moreover, PPCa was also supported onto the surface of nano-$CaCO_3$ to further improve the dispersion and nucleating efficiency in PLLA matrix.[26]

Till now, various types of nanofillers have been used for the preparation of composites with different types of environmentally friendly polymer resins.[27-30] However, nanocomposites based on PLLA and montmorillonite (MMT) have attracted great interest in today's materials research, because the properties of these nanocomposites can be significantly improved especially when compared with neat PLLA. These improvements can include high moduli, increased strength, flexibility, and heat resistance, decreased gas permeability and flammability, and control of degradability. However, interest crystallization behaviors of organoclay reinforced PLLA nanocomposites were observed.[31] Bulk kinetics studies and radial spherulite growth rates indicate that when a high degree of filler polymer matrix miscibility is present, nucleation properties of the organoclay are low relative to the less miscible organoclay. Therefore, the overall bulk crystallization rate was increased in the intercalated system and somewhat retarded in the exfoliated system. Compared to the NAs aforementioned, MMT is a less efficient nucleating agent for PLA as the reduction in $t_{1/2}$ is moderate in isothermal mode and it is not effective for high cooling rates in non-isothermal crystallization. Hence, it is of great importance to develop PLLA/MMT nanocomposites with improved crystallization properties.

In this work, a novel montmorillonite with nucleating surface (NMMT) for enhancing crystallization of PLLA was synthesized by the reaction between phenylphosphonic acid and the calcium ion on the surface of a Ca-montmorillonite (MMT). Then the NMMT was introduced into PLLA as the nucleating agent by the melt blending method. A comparative study on the nucleation ability of NMMT was done with that of PPCa and talc. The structure of NMMT coated with PPCa surface was proved by DSC, FTIR and WAXD. The nonisothermal, isothermal crystallization behavior and spherulite morphology of PLLA/NMMT blends with different MMT/PPOA mass ratio and NMMT fraction were investigated. Finally, the effects of the addition of NMMT as well as heat treatment on the static and dynamic mechanical properties of PLLA were observed. The supported MMT with high surface area may not only disperse nucleating agent active component effectively and increase the efficiency, and reduce the cost of nucleating agent, but also increase the strength and modulus of nucleated PLLA due to the reinforce of MMT.

Experimental

Materials

The PLLA used in this study was supplied by Zhejiang Hisun Biomaterials Co. Ltd.. It had a density of 1.25 g cm^{-3}, a weight-average molecular weight (M_w) of 134 kg mol^{-1} and a polydispersity of 1.9 (GPC analysis). The DK4 Ca-montmorillonite (MMT) modified by cetyl quaternary ammonium was purchased from Zhejiang Fenghong Clay Chemicals Co., Ltd. DK4 nanoclay is comprised of 52 wt% montmorillonite (TGA analysis). Phenylphosphonic acid (PPOA) with a melting point of about 166 ^{o}C was purchased from Jiaxing Alpharm Fine Chemical Co. Ltd., China. Talc (1250 mesh) without any surface pre-treatment was purchased from Dashiqiao City Fuhua Mining Co. Ltd. in China. All of these chemicals were used as received. Calcium phenylphosphonic acid (PPCa) was prepared according to previous work [25].

Preparation of MMT with nucleating surface

MMT and PPOA were dried in a vacuum oven at 80 ^{o}C for 4 hours. After that, they were well mixed directly at room temperature. Then, the powder was placed in an oven to fully react at 180 ^{o}C for 5 min. The MMT prepared by MMT/PPOA mass ratios of 5/1, 10/1, 20/1 and 40/1, was denoted as M_5, M_{10}, M_{20} and M_{40}. Untreated MMT was denoted as M_0.

Preparation of PLLA/NMMT nanocomposites

PLLA, MMT, PPCa, Talc and NMMT were dried in a vacuum oven at 110 ^{o}C for 4 hours before melt blending. PLLA/NMMT blends were prepared using a Haake Rheomix 600 internal mixer. The melt compounding of PLLA with NMMT was performed at 175 ^{o}C for 8 min, with a rotor speed of 50 rpm, and the total mixing weight per batch was ca 60 g. For comparison, neat PLLA, PLLA/MMT, PLLA with 2 wt% PPCa and 2 wt% talc (denoted as PLLA/PPCa2 and PLLA/talc2, respectively) were treated using the same procedure. Nanocomposite filled by MMT and NMMT was denoted as XPM_0 and XPM_n, where X representing the content of NMMT or MMT (wt%) of the composite, and n representing the mass ratio of MMT/PPOA.

Characterization

The molecular weight parameters of neat PLLA and $5PM_5$ were measured by gel permeation chromatography (GPC) using a Waters instrument (515 HPLC) equipped with a Waytt interferometric refractometer. GPC columns were eluted with $CHCl_3$ at 25 ^{o}C at 1 mL min^{-1}. The molecular weights were calibrated with polystyrene standards. After melt processing, the molecular weights of neat PLLA and $5PM_5$ were investigated. The M_w values of neat PLLA and $5PM_5$ are 121 and 115 kg mol^{-1} with M_w/M_n values of 1.83 and 1.88, respectively. The molecular weight parameters characterization confirms that, under processing conditions, melt blending of PLLA with NMMT does not induce any dramatic drop of PLLA weight average molar mass by thermal degradation or hydrolysis of the polyester chains.

The FTIR measurements were carried out on a BIO-Rad Win-IR spectrometer. The spectrum was recorded in the range of 500-4000 cm^{-1} with a resolution of 4 cm^{-1}.

The crystallization behavior and melting characteristics of

PLLA and its blends were carried out using a TA instruments differential scanning calorimeter (DSC) Q20 with a Universal Analysis 2000. Indium was used for temperature and enthalpy calibration. All operations were performed under nitrogen purge,
5 and the weight of the samples varied between 5 and 8 mg. In the case of nonisothermal melt crystallization, the samples were heated from ambient temperature to 190 ^{o}C at a heating rate of 100 ^{o}C min^{-1}, held for 2 min to erase the thermal history and then cooled to 40 ^{o}C at a cooling rate of 10 ^{o}C min^{-1} and then reheated
10 to 190 ^{o}C at the same rate to investigate the subsequent melting behavior. For the investigation of isothermal crystallization, the samples were initially melted at 190 ^{o}C for 2 min to ensure completely amorphous state, and then rapidly cooled to the desired crystallization temperature (T_c) at a rate of 45 ^{o}C min^{-1}. It
15 is worth noting that all recorded crystallization and melt enthalpies were normalized according to the amount of PLLA within the blend.

Wide-angle X-ray diffraction (WAXD) patterns of the samples were characterized using a Rigaku model Dmax 2500 X-ray
20 diffractometer. The Cu Kα radiation (λ = 0.15418 nm) source was operated at 40 kV and 200 mA. The scanning angle (2θ) covered a range of 10-30° for PLLA/NMMT blends at a speed of 3 ^{o} min^{-1}, respectively.

An optical microscope (POM) (Leica DM2500 P) equipped
25 with a temperature controller (Linkam LTS 350) was used to investigate the spherulitic morphology. Samples were first annealed at 190 ^{o}C for 2 min to erase any thermal history. Then they were quickly cooled to the desired temperature for isothermal crystallization. After the completion of crystallization,
30 the spherulite morphologies were recorded.

Tensile properties were measured on an Instron-1121 tensile tester in accordance with the standard ISO 527-93 at a crosshead speed of 2 mm min^{-1}. The specimens were prepared into dumbbell type with dimensions of 80 mm (total length) × 10 mm
35 (width) × 4 mm (narrow portion width) × 1.0 mm (thickness) by hot compression molding. The specimens were hot-pressed at 180 ^{o}C and 10 MPa for 5 min, followed by a quenching into ice water. To examine the influence of annealing on mechanical properties, a part of the specimens were heat-treated at 130 ^{o}C for 2 min in a
40 convectional oven. An average value on at least five tests was taken for each specimen.

Dynamic mechanical analysis (DMA) was performed on the samples of 20.0 × 4.0 × 1.0 mm^3 in size using a dynamic mechanical analyzer from Rheometric Scientific under tension
45 mode in a temperature range of 20 to 120 ^{o}C at a frequency of 1 Hz and 3 ^{o}C min^{-1}.

Results and discussion

### Characterization of MMT with nucleating surface by DSC，FTIR and WAXD

50 In order to prove the formation of PPCa chemically supported on the surface of MMT, neat PPOA and MMT with various MMT/PPOA mass ratios are qualitatively characterized by DSC, shown in Fig. 1 (a). It can be observed that the PPOA has a melting peak at 166 ^{o}C with a melt enthalpy being around 146.3 J
55 g^{-1}. For PPOA supported on MMT, no discernible melting peaks of PPOA are observed during heating process. It is suggested that the chemical reaction took place between MMT and PPOA to
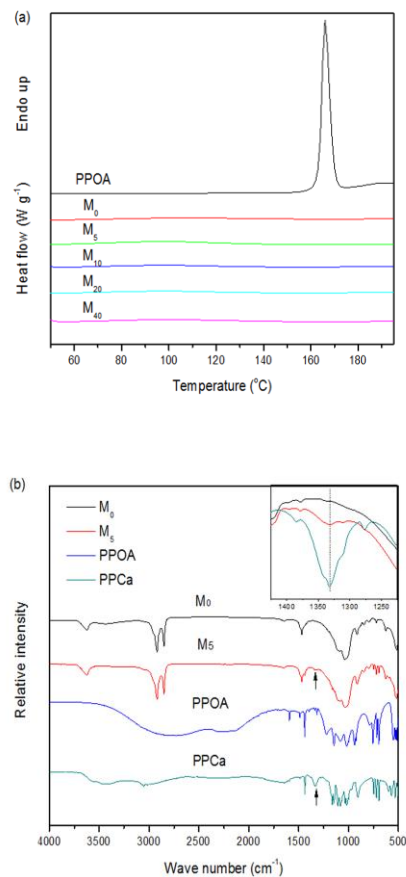
formation of PPCa on the surface of MMT. Then, the samples of
Figure 1. (a)DSC heating curves of PPOA and PPOA supported on MMT
60 with various MMT/PPOA mass ratio at a heating rate of 10 ^{o}C min^{-1}; (b) FTIR spectrum of M$_0$, M$_5$, PPOA and PPCa at room temperature.

M$_0$, M$_5$, PPOA and PPCa at room temperature are further qualitatively characterized by FTIR as shown in Fig. 1 (b). Before the FTIR measurements, the M$_5$ sample was washed by acetone
65 three times. For the M$_0$, the characteristic bands at 2851-2919 cm^{-1} and 1469 cm^{-1} are attributed to the C-H stretching and bending vibration, respectively. The band at 1037 cm^{-1} is due to Si-O stretching vibration and the bands at 519 cm^{-1} stands for Al-O-Si structure.[32] For the PPOA, the P-C stretching band characteristic
70 of the P-C$_6$H$_5$ group and the P=O stretching band are present at 1439 cm^{-1} and 1222 cm^{-1}, respectively.[33] In addition, the C-H out-of-plane deformation bands of the monosubstituted benzene ring are located at 756 and 696 cm^{-1}, respectively. In the FTIR spectrum of PPCa, the characteristic bands at 1439 cm^{-1} and 690-
75 770 cm^{-1} are correspond to the dissymmetry and symmetry stretching vibration of phenyl of PPCa. The characteristic bands at 1335 cm^{-1} may be corresponding to the stretching vibration of COO– of PPCa. Compared to the spectrum of PPCa, the prepared PPCa supported on the surface of MMT (NMMT) shows
80 characteristic bands at 695 cm^{-1}, 749 cm^{-1} and 1439 cm^{-1}, which are assigned to the stretching vibration of C-H and P=O of the formed PPCa, respectively. Compared to the spectrum of PPCa, the prepared NMMT shows characteristic bands at 1335 cm^{-1},

which are assigned to the stretching vibration of COO– of PPCa. This result indicates that the PPOA adheres on the surface of MMT reacting with the metal ion mainly to form an unextractable PPCa layer on the surface of MMT. A very similar result was
5 also reported previously,[34,35] in which a MMT with β-nucleating surface for polypropylene supported by chemically calcium

(a)

(b)
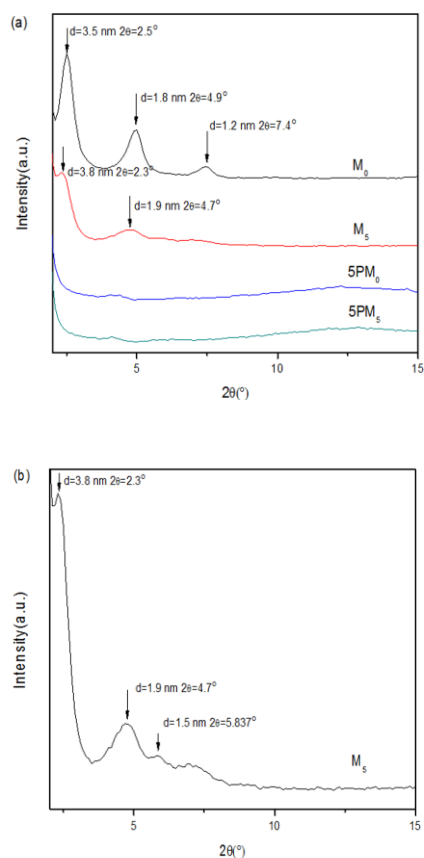
pimelate was prepared through the chemical reaction between pimelic acid and calcium ion on the surface of the same Ca-MMT. Figure 2. The WAXD profiles of (a)M0, M5, 5PM0 and 5PM5
10 and (b)M5.

Fig. 2 shows the WAXD patterns of M_0, M_5, $5PM_0$ and $5PM_5$. For M_5 sample in Fig. 2 (b), a peak at $2\theta = 5.8^{o}$ can be clearly observed due to the d_{001} equidistance of PPCA [25], further
15 indicating the formation of PPCA on the surface of MMT. Moreover, the mean interlayer spacing of the (001) plane (d001) for the MMT obtained by WAXD measurements is 3.5 nm ($2\theta = 2.5^{o}$), accompanied with the appearance of a peak at $2\theta = 4.9^{o}$, which is due to d_{002} equidistance. The interlayer spacing, d(001),
20 of the M_5 (3.8 nm) was slightly higher than that of the d(001) of M_0 (3.5 nm). Therefore, the reaction occurred mainly inside the MMT layers with diffusion of the PPOA molecules to penetrate into the inter-space and react with the calcium ion inside the clay sheets. In the case of PLLA/MMT and PLLA/NMMT
25 nanocomposites, the peak at (001) plane (d001) disappear, and that at (002) plane (d002) shifts from $2\theta=4.9^{o}$ to $2\theta=4.2^{o}$ and the

intensity of the peaks is much more attenuated, indicating the formation of intercalated and/or exfoliated structure. In contrast to PLLA/MMT nanocomposite, the intensity of the peaks at (002)
30 plane (d002) of the PLLA/NMMT nanocomposites is very similar, indicating the reaction of PPOA on the surface of MMT does not affect its dispersion state in the PLLA matrix.

Nonisothermal crystallization and melting behavior of PLLA nanocomposites filled by MMT with nucleating surface
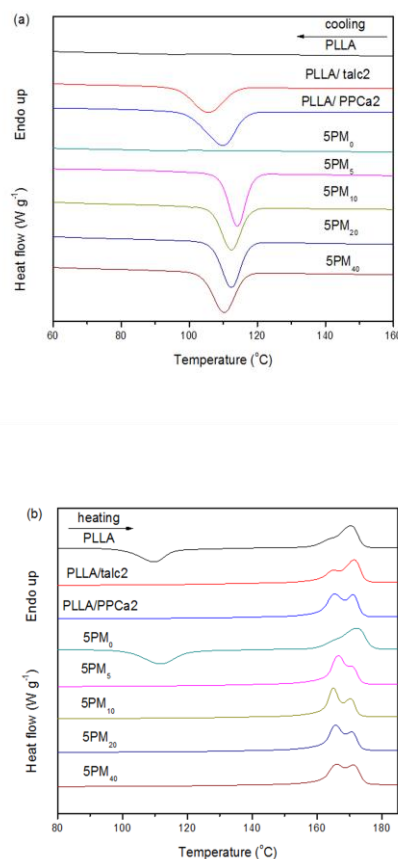
35

(a)

(b)

Figure 3. DSC curves of (a) nonisothermal crystallization and (b)
subsequent melting for pure PLLA, PLLA/talc2, PLLA/PPCa2,
40 PLLA/MMT and PLLA/NMMT blends. Both the cooling and heating rates are 10 oC min-1.

DSC analysis was taken to compare the effect of NMMT, MMT, PPCa and talc on the crystallization behavior of PLLA.
45 Fig. 3 shows the nonisothermal crystallization and subsequent melting curves of neat and nucleated PLLAs. The parameters of interest, such as crystallization temperature (T_c), crystallization enthalpy (ΔH_c), melting temperature (T_m), melting enthalpy (ΔH_m), and crystallinity (X_c) are summarized and listed in Table
50 1. The values of X_c are estimated from the relation $X_c = \Delta H_c / \Delta H^{o}_m \times 100\%$, where $\Delta H^{o}_m = 93$ J g^{-1} is the melting enthalpy of 100% crystalline PLLA [36-38]. As seen in Fig. 3, pure PLLA and PLLA/MMT nanocomposite display very slow crystallization kinetics. Upon cooling at 10 ^{o}C min^{-1}, no discerned

crystallization peak can be observed, and cold crystallization peaks appear at 109.9 and 112.1 ^{o}C, respectively, in the following heating scans, indicating somewhat retarded effect of MMT on the crystallization of PLLA as reported previously.[31] Usually, a high T_c with a narrow crystallization temperature range observed under cooling conditions reflects faster crystallization rate. With the addition of 2 wt% talc or PPCa, a broad crystallization peak appears in the DSC cooling curve. Both talc and PPCa can promote the crystallization of PLLA, due to the fact that the samples crystallize well in the cooling process. For the NMMT-nucleated PLLA sample with 10 wt% M_5, the crystallization exothermal peak becomes much sharper and shifts to a higher temperature by ca. 10.8 ^{o}C and 6.0 ^{o}C in comparison with PLLA containing 2 wt% of talc and PPCa, respectively. In addition, the value of X_c increases to 46.9% with the incorporation of NMMT, compared to 33.1% for talc and 41.7% for PPCa. All of these results indicate that NMMT accelerates the crystallization of PLLA more significantly, and its nucleation activity is much greater than that of talc or PPCa. From Fig. 3(b), it is found that two melting peaks appear in the heating scan for the PLLA/NMMT and PLLA/PPCa samples, while only one for neat PLLA and PLLA/MMT. The different melting behavior of PLLA is mainly dependent on crystallization temperature, and the double endothermal peaks shown here can be due to the melt-recrystallization mechanism. The lower temperature peak is attributed to melting of primary crystals, and the higher one corresponds to melting of recrystallized crystals.

The effect of NMMT content on the crystallization and melting behavior of PLLA was also investigated by DSC. Fig. 4 shows the nonisothermal crystallization and reheating curves of PLLA/NMMT blends with various M_5 contents. It is found that the crystallization of PLLA becomes faster and T_c increases progressively with increasing M_5 content from Fig. 4(a). It is well known that the crystals formed at higher T_c always have higher T_m and X_c, due to the fact that the lamella is thickened by increasing T_c. Because of the ascent of the crystallization temperature range, the values of T_m and X_c increase monotonously with an increase of M_5 content, as is revealed in Fig. 4(b) and Table 1.
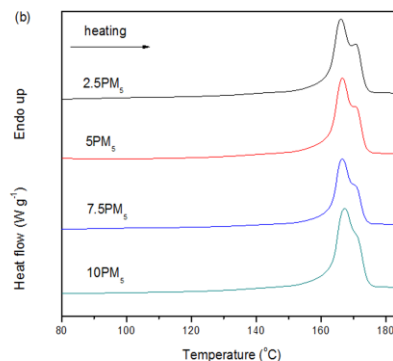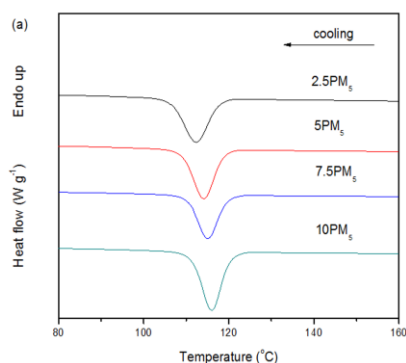

Figure 4. DSC curves of (a) nonisothermal crystallization and (b) subsequent melting for PLLA/NMMT blends with different M_5 contents. Both the cooling and heating rates are 10 ^{o}C min^{-1}.

Table 1. Nonisothermal crystallization and melting parameters of pure PLLA and its blends.

Samples	T_c (^{o}C)	ΔH_c (J g^{-1})	T_m (^{o}C)	ΔH_m (J g^{-1})	X_c (%)
PLLA	_	0	163.5,170.3	33.7	0
PLLA/2% talc	105.4	30.8	165.2,171.4	38.1	33.1
PLLA/2%PPCa	110.2	38.8	165.2,171.1	45.2	41.7
5PM_0	_	0	165.1,172.3	36.9	0
5PM_{40}	110.2	35.3	166.3,171.6	42.6	38.0
5PM_{20}	112.3	36.3	165.7,170.8	42.9	39.0
5PM_{10}	112.4	36.4	165.2,170.2	43.0	39.1
2.5PM_5	112.3	39.6	166.2,170.8	42.1	40.6
5PM_5	114.2	38.4	166.6,170.8	44.2	41.3
7.5PM_5	115.1	40.4	166.7,170.9	44.2	43.4
10PM_5	116.2	43.6	167.3,171.0	48.5	46.9

Isothermal crystallization

The completion of isothermal crystallization inside the preheated mold over a short cycle period is very important for the efficient injection molding of high performance PLLA articles. In this concern, the isothermal crystallization behavior of PLLA containing the three kinds of different NAs was explored. Fig. 5 shows the DSC curves of neat and nucleated PLLAs crystallized at 140 ^{o}C. Obviously, at such a low under cooling, the crystallization rate of pure PLLA and PLLA/MMT is very slow, even by incorporating 2 wt% talc. With the addition of NMMT and an increase of its content, the exothermal peak sharpens and

increases in amplitude. The relative crystallinity (X_t) at a given crystallization time (t) can be calculated from the integrated area
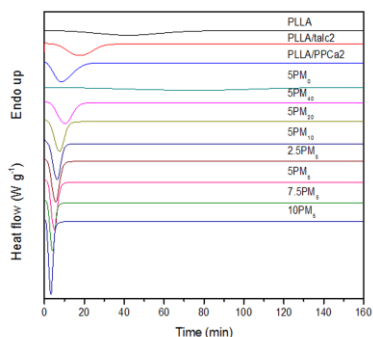

Figure 5. DSC exotherms of isothermal crystallization at 140 oC for pure PLLA, PLLA/talc2, PLLA/PPCa2, PLLA/MMT and PLLA/NMMT blends.
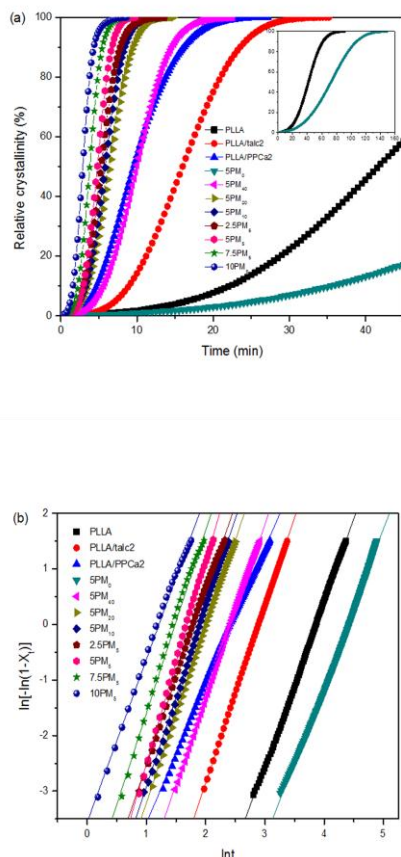

Figure 6. (a) Conversion curves and (b) Avrami plots of pure PLLA, PLLA/talc2, PLLA/PPCa2, PLLA/MMT and PLLA/NMMT blends isothermally crystallized at 140 oC.

of the DSC curve from $t = 0$ to t divided by the whole area of the exothermal peak. The conversion curves of X_t versus t for neat PLLA and its blends crystallized at 140 ^{o}C are presented in Fig. 6(a). All the curves exhibit a sigmoid dependence on time. As can be seen from the inset of Fig. 6(a), pure PLLA and PLLA/talc2 complete the crystallization within 90 and 35 min, respectively. In contrast, the addition of PPCa or NMMT can effectively enhance the isothermal crystallization of PLLA, and the effect is even more pronounced for NMMT.

The Avrami equation is frequently employed to analyze the isothermal crystallization kinetics of polymers, according to the dependence of X_t (the crystallized fraction) in the crystallization time [39, 40]:

$$1- X(t) = \exp(- k\, t^n) \qquad (1)$$

where n is the Avrami exponent dependent on the nature of nucleation and growth geometry of the crystals, and k is the overall rate constant associated with both nucleation and growth contributions. The linear form of Eq. 3 can be expressed as follows:

$$\ln[-\ln(1-X_t)]=\ln k +n\ln t \qquad (2)$$

The Avrami parameters n and k can be obtained from the slopes and the intercepts, respectively. Fig. 6(b) shows such plots for the samples isothermally crystallized at 140 ^{o}C. The crystallization half-time $t_{1/2}$, which is defined as the half period (i.e. 50% crystallization) from the onset of crystallization to the end of crystallization, is an important parameter for the discussion of isothermal crystallization kinetics. The value $t_{1/2}$ comes from eq(1), putting in it; $X(t) = 1/2$ and $t = t_{1/2}$; then one obtains:

$$t_{1/2}=(\ln2/k)^{1/n} \qquad (3)$$

The values of n, k and calculated $t_{1/2}$, are listed in Table 2. The value of n fluctuates within the range of 2.3-3.6, and is almost irrespective of the addition of NAs, reflecting the formation of spherulites, heterogeneously nucleated. On the basis of the data of k and $t_{1/2}$, it is evident that the nucleation ability of the three NAs increases following the order: talc < PPCa < NMMT.

Table 2 also shows the effects of NMMT content and isothermal crystallization temperature (T_c) on $t_{1/2}$ of PLLA. With increasing T_c from 130 to 140 ^{o}C, the crystallization of pure PLLA becomes difficult and $t_{1/2}$ is prolonged because the excessive mobility of macromolecular chain restricts the nucleation process at high temperature. A similar situation is also found for the PLLA/MMT nanocomposite. However, at a given T_c, $t_{1/2}$ of PLLA decreases by 1-2 orders of magnitude with the addition of NMMT, and displays a continuously downward tendency when the mass ratio of MMT/PPOA is decreased and the NMMT amount is increased. It should be pointed out that NMMT could induce the rapid crystallization of PLLA at lower under cooling (i.e. $T_c > 140$ ^{o}C), indicative of a great nucleation ability of NMMT. It is reported that the optimal temperature range for molding PLLA is between 100 and 110 ^{o}C in order to obtain sufficient degree of crystallinity within a short time interval [41]. As a matter of fact, the value of $t_{1/2}$ for the PLLA/NMMT sample crystallized at 110 ^{o}C is difficult to determine due to the rapid crystallization rate. Thus, it is reasonable to speculate that NMMT can serve as a powerful nucleating agent for fast molding of PLLA articles in practical processing.

Table 2. Kinetic parameters of pure PLLA and its blends isothermally crystallized at different temperatures.

Sample	$T_c(^{o}C)$	n	k (min^{-n})	$t_{1/2}$ (min)
PLLA	140	2.9	1.16×10^{-05}	41.7
	135	2.9	8.19×10^{-05}	22.9
	130	2.5	2.18×10^{-03}	10.1
PLLA/2% talc	140	3.2	1.03×10^{-04}	16.0
	135	2.8	2.49×10^{-02}	7.21
	130	2.9	0.03447	1.82
PLLA/2%PPCa	140	2.9	6.66×10^{-04}	9.78
	135	3.0	4.98×10^{-03}	4.84
	130	2.9	0.032	2.39
5PM$_0$	140	2.8	4.85×10^{-06}	70.1
	135	2.9	1.22×10^{-05}	44.1
	130	3.0	5.90×10^{-05}	22.7
5PM$_{10}$	140	3.4	1.46×10^{-03}	6.25
	135	2.7	4.19×10^{-02}	2.88
	130	2.7	0.70	0.99
5PM$_{20}$	140	3.0	2.39×10^{-03}	6.46
	135	3.2	2.30×10^{-02}	2.89
	130	2.4	0.40	1.25
5PM$_{40}$	140	3.1	5.29×10^{-04}	10.0
	135	2.5	3.04×10^{-02}	3.45
	130	2.8	0.29	1.37
2.5PM$_5$	140	3.3	2.96×10^{-03}	5.34
	135	2.8	5.72×10^{-02}	2.46
	130	2.6	0.98	0.85
5PM$_5$	140	3.6	2.14×10^{-03}	4.89
	135	2.7	0.10	1.99
	130	2.3	1.19	0.79
7.5PM$_5$	140	3.3	7.57×10^{-03}	3.95
	135	2.8	0.13	1.83
	130	2.3	1.67	0.66
10PM$_5$	140	2.9	1.72	2.90
	135	3.3	7.96×10^{-04}	1.42
	130	2.3	1.97	0.62

Spherulite morphology

The polarized optical microscopy (POM) was a visual method for monitoring the growth and morphology of polymer spherulites and it was used in the present study. Fig. 7 shows the POM images of PLLA and its blends with MMT and various NAs after isothermal crystallization at 130 ^{o}C. Since the amount of the nuclei is quite few in pure PLLA, the spherulites grow hugely and collide with each other, of which the diameter reaches up to about 100 um. For PLLA/MMT sample, due to the retarded effect of MMT on the crystallization, the spherulite size is slight larger than that of neat PLLA. Upon addition of 2 wt% talc or PPCa, the diameter of the spherulites is reduced to approximate 10 um or less, and the spherulite size of the PLLA/PPCa2 sample, which has a nonuniform distribution, is slightly smaller than the one of PLLA/talc2. As for NMMT-nucleated PLLAs, very fine crystals with blurry boundaries are observed and the nucleation density is increased with increasing NMMT content. By comparing the effect of the three NAs on the crystalline morphology of PLLA, it is apparent that NMMT can provide the largest number of nuclei. The POM analysis further confirms that NMMT has the more prominent efficiency on inducing the crystallization of PLLA than talc and PPCa, which is well consistent with the aforementioned DSC results.
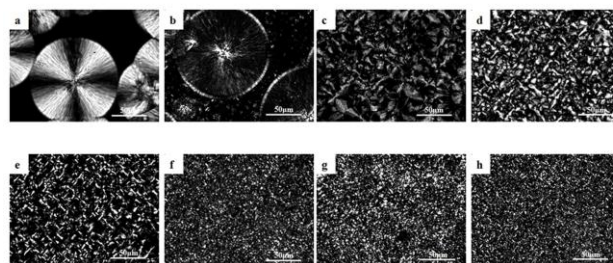

Figure 7. POM photographs of pure PLLA and its blends isothermally crystallized at 130 oC. (a)PLLA; (b)5PM0; (c)PLLA/talc2; (d)PLLA/PPCa2; (e)2.5PM5; (f)5PM5; (g)7.5PM5; (h) 10PM5.

Discussion on nucleating mechanism

Till now, two main mechanisms, namely chemical nucleation and epitaxial nucleation have been widely proposed to explain the nature of nucleation phenomena of polymers nucleated by NAs. Concerning the chemical nucleation, a chemical reaction between the polymer and NA occurs, leading to the formation of a new nucleating compound which plays the role of the true nucleating species. According to the chemical structure and previous works,[24, 25] a chemical reaction is not expected to occur between metal phosphonates and PLLA, and thus the possibility that the nucleation of NMMT-containing PLLA induced by the chemical mechanism could be ruled out.

As far as epitaxial nucleation is concerned, the polymer chains epitaxially grow on the surface of NA, and the matching between the two crystal structures of polymer and NA does matter.[42-45] Therefore, the crystal structure of PPCA was analyzed and compared with that of PLLA. As reported by Stone et al.,[46] the single crystal of the PPCa complex has a monoclinic unit cell with lattice parameters a =31.27 Å, b =5.61 Å, c =7.72 Å. In the PLLA α crystal, the chains pack in an orthorhombic or pseudoorthorhombic unit cell with dimensions a =10.34 Å, b = 5.97 Å, and c = 28.8Å.[47] The length of the a-axis of PPCa

crystal is thrice that of the a-axis of PLLA crystal, with a tiny misfit of 0.79%. In the PPCa monoclinic unit cell, one has to consider not only the linear parameters a, b and c, but also the angle β = 101.92^o. This is very important because the equidistance $4 \times d_{001}$ = $4 \times c_0 sen\beta$ = 30.21 Å is not quite dissimilar from the parameter c_0 = 28.8 Å of the orthorhombic PLLA α crystal. Hence the maximum corresponding misfit m= [(30.21- 28.8)/28.8] is quite low: 4.8%. This proves that there are two good misfit: the one, m_1 = 0.79% and the second one m_2 = 4.8% which give rise to a nice 2D coincidence lattice in the 010 plane of both structures. Moreover, looking at the difference between the two b_0 parameters, one obtains: m_3 = (5.97- 5.61) / 5.61= 6.4%. The three misfits are really compatible with the Royer's conditions for the epitaxy. Therefore the two structures are epitaxially related on three planes: 100, 010 and 001. Due to the excellent matching between these lattice parameters, it is presumed that PLLA crystals might grow on the surface of PPCa by an epitaxial mechanism. It should be noted that the layered structure of PPCa and PPZn is very similar, while dimensions of unit cell are very different. The PPZn crystal possesses an orthorhombic cell with lattice parameters a =5.66 Å, b =14.45 Å, c =4.8 Å. The length of the c axis of the PLLA a crystal is twice that of the b axis of the PPZn crystal, with a tiny mismatching of 0.3%.[24] Hence it was proposed that PLLA crystals might grow on the PPZn surface with the (001) lattice plane of PLLA along the (010) direction of PPZn crystals. Moreover, due to the hydroxyl groups in NMMT (as seen in Fig. 1) and the carbonyl groups in PLLA chains, hydrogen bond interaction between NMMT and PLLA might act as a template to adsorb the molecular chains, as suggested in previous work.[20] Accordingly, the potential hydrogen bonding interactions between the hydroxyl groups of NMMT and the carbonyl groups in PLLA chains could stabilize the nucleation process. The benzene rings of the PPCa may also act as a growth surface of crystal and induce PLLA chains epitaxial crystallize on it.[48] However, additional investigation is still needed for an in-depth understanding of the exact nucleation mechanism. In contrast to PPCa, the great nucleation ability of NMMT to accelerate the crystallization of PLLA can be explained by the fact that NMMT possesses the larger specific surface area as illustrated in Fig. 8.
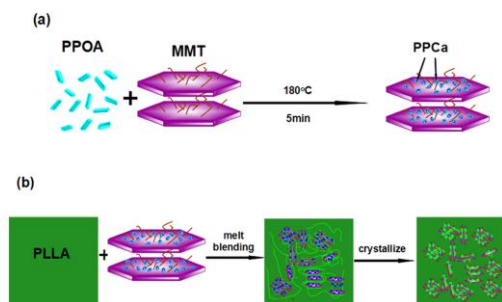

Figure 8. Schematic diagrams of prepared PLLA/NMMT nanocomposites.

Mechanical properties

The tensile properties of pure PLLA and PLLA/NMMT blends were investigated. The typical stress versus strain curves of the
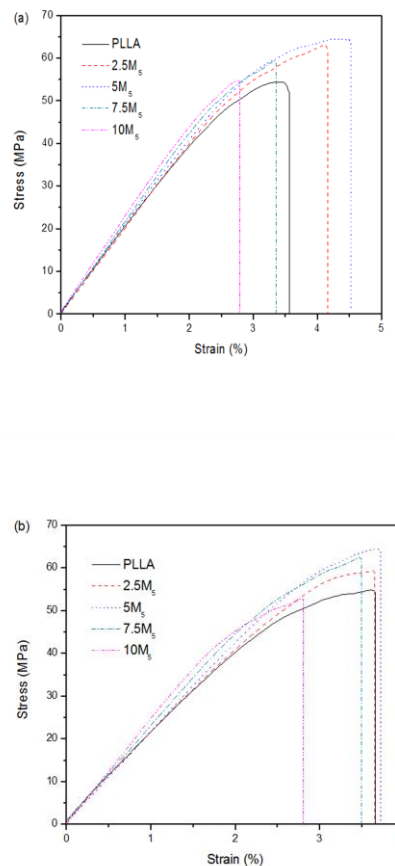

Figure 9. Typical stress versus strain curves of pure PLLA and PLLA/NMMT blends, (a) without annealing; (b) annealed at 130 oC for 2 min.

quenched and subsequently annealed specimens are shown in Fig. 9. The corresponding tensile strength, Young's modulus and elongation at break are summarized and listed in Table 3. Neat PLLA shows a tensile strength of 54.1 MPa, a modulus of 2.01 GPa, and an elongation at break of 3.6%. As seen in Table 3, the tensile strength increases to 64.3 MPa with the addition of 5% NMMT. This is possibly due to that the interaction force between montmorillonite layers is very strong, the activity of PLLA molecular chains which between the layers is constrained. The effect of interface is obvious due to the large specific surface area of montmorillonite. The montmorillonite layers in PLLA matrix is equivalent to the role of the crosslinking points, lead to the increase of the PLLA strength. Nevertheless, there is a decrease in the tensile strength afterward when the NMMT content is higher than 5 wt%. A possible explanation is due to the filler aggregation. However, with the amount of filler more than 5 wt%, the dispersibility and compatibility decrease and the probability of aggregation increases, thus less energy is required

to propagate the cracks come into being.[49] During the tensile testing, the stress can not transfer effectively nearby these aggregations, resulting in decrease of the tensile strength. Hence, increasing the amount of NMMT within a certain value increases the tensile strength.

After annealing at 130 °C for 2 min, pure PLLA does not show pronounced changes in its tensile properties, whereas for PLLA/NMMT blends, the tensile strength and modulus are enhanced, and the elongation is close to pure PLLA as can be seen from Fig. 9(b) and Table 3. Fig. 10 shows the diffraction curves of PLLA and PLLA/NMMT blends. The samples for the WAXD experiment were the annealed specimens employed in the tensile tests. It is found that pure PLLA remains nearly amorphous after the heat treatment. To the PLLA/NMMT blends, strong peaks can be observed at $2\theta = 16.5$ ° and 18.7 °, corresponding to (200)/(110), and (203), which are the typical diffraction peaks of α form as reported previously, indicating that NMMT can highly enhance the crystallization rate of PLLA. Taking the results from Fig. 10 into account, it should be believed that the increase of tensile strength and modulus, as well as the decrease of elongation come from the rapid crystallization of NMMT-nucleated PLLAs in such a short annealing time.

Table 3. Static Mechanical Properties of PLLA and its blends with M_5

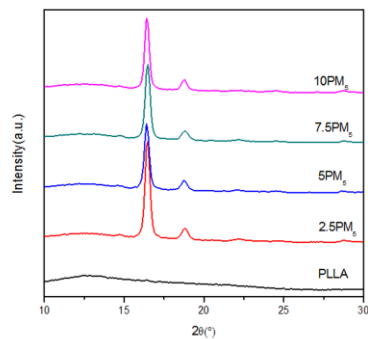| Sample	Heat treatment [a]	Tensile strength (MPa)	Young's modulus (GPa)	Elongation at break (%)
PLLA	None	54.1±2.5	2.01±0.07	3.6±0.5
	Annealed	54.6±2.0	2.03±0.09	3.7±0.7
2.5M_5	None	59.7±1.5	2.01±0.04	4.0±0.2
	Annealed	59.9±1.7	2.07±0.13	3.6±0.4
5M_5	None	64.3±2.1	2.06±0.03	4.5±0.6
	Annealed	64.5±3.7	2.20±0.05	3.7±0.5
7.5M_5	None	59.3±2.5	2.11±0.03	3.3±0.3
	Annealed	62.4±3.5	2.45±0.02	3.2±0.3
10M_5	None	54.9±2.8	2.20±0.06	2.8±0.7
	Annealed	55.2±2.9	2.51±0.02	2.7±0.6

Figure 10. WAXD patterns of pure PLLA and PLLA/NMMT blends annealed at 130 oC for 2 min.

The dynamic mechanical properties of the annealed samples were also investigated by DMA under the tension mode. Fig. 11 shows the temperature-dependent storage modulus (E') of pure PLLA and NMMT-nucleated PLLAs. It is clear that the storage modulus of PLLA/NMMT blends is higher than that of pure PLLA at low temperature in the glassy state, indicating that an enhanced stiffness is accomplished by the addition of NMMT. For example, the value of E' is 2.85 GPa for pure PLLA at 25°C, which increases to 3.06, 3.29, 3.41 and 3.59 GPa, respectively, with increasing the NMMT content from 2.5 to 10 wt%. Both pure PLLA and PLLA/NMMT blends show a sharp reduction in E' at about 60 °C, corresponding to the glass transition of PLLA (T_g). At temperatures higher than 100 °C, the E' of pure PLLA increases slightly, which is attributed to the occurrence of cold crystallization. Due to the existence of crystalline phase formed after heat treatment, the NMMT-nucleated samples also exhibit a much higher modulus than that of pure PLLA at temperatures above T_g, suggesting that the PLLA/NMMT blends may possess a better heat resistance. On the basis of these results, it can be concluded that NMMT is an effective nucleating agent to induce the rapid crystallization of PLLA and simultaneously improve its mechanical properties through a short-period annealing procedure.
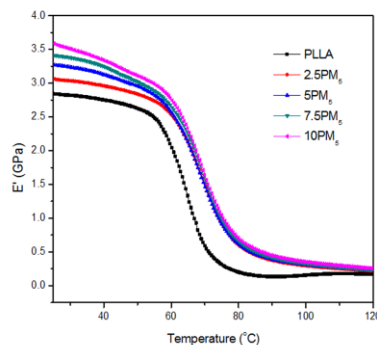
Figure 11.Temperature dependence of storage modulus for pure PLLA and PLLA/NMMT blends after heat treatment.

Conclusions

A novel montmorillonite with nucleating surface (NMMT) supported by chemically PPCa for enhancing crystallization of PLLA were synthesized and then incorporated into PLLA by melt blending. The crystallization, melting behavior and mechanical properties of the resultant blends were investigated in detail. DSC results show that NMMT significantly accelerates the nonisothermal and isothermal crystallization of PLLA from the melt. With the addition of 2.5 wt% NMMT with a MMT/PPOA mass ratio of 40:1, PLLA could complete the crystallization under cooling at 10 ^{o}C min^{-1}, and the crystallization half-time decreases remarkably, with this effect being more prominent as increasing NMMT content and decreasing MMT/PPOA ratio. POM observation indicates that NMMT provides a large number of nucleation sites for the crystallization of PLLA and leads to an apparent reduction of the spherulite size. On the basis of the crystal parameters of PLLA and PPCa, the nucleation phenomenon of PLLA/NMMT system is suggested to be caused by epitaxial mechanism. Furthermore, the addition of NMMT increases the tensile strength and modulus of the amorphous PLLA. After annealing at 130 ^{o}C for 2 min, both the tensile and storage modulus of PLLA are improved by the presence of NMMT. Consequently, it is considered that NMMT is a new efficient nucleating agent for improving the thermomechanical properties and processability of PLLA, which may be of great interest for expanding the application fields of PLLA-based nanocomposites.

Acknowledgment

Notes and references

^{a}Key Laboratory of Polymer Ecomaterials, Changchun Institute of Applied Chemistry, Chinese Academy of Sciences, Changchun 130022, China, E-mail: cyhan@ciac.ac.cn; Fax: +86-431-85262244.
^{b}College of Chemistry, Xiangtan University, Xiangtan 411105, Hunan Province, P. R. China

1. J. J. Yang, Y. R. Liang, W. C. Shi, H. S. Lee, C. C. Han. Polymer, 2013; 48: 3974-3981.
2. D. H. Zhang, M. A. Kandadai, J. Cech, S. Roth, S. A. Curran. J. Phys. Chem. B, 2006**;** 110: 12910-12915.
3. A. Rafael, H. Bruce, S. Susan. Macromol. Biosci., 2004; 4: 835–864.
4. S. Cedric, R. Jean-Marie, D Philippe. ACS Appl. Mater. Inter., 2013**;** 22: 11797–11807.
5. J. R. Sun, J. Shao, S. Y. Huang, B. Zhang, G. Li, X. H. Wang, X. S. Chen. Materials letter., 2012; 89: 169-171.
6. S. Yoshimoto, T. Ueda, K. Yamanaka, A. Kawaguchi, E. Tobita, T. Haruna. Polymer, 2001; 42: 9627-9631.
7. B. Lotz, J. C. Wittmann, W. Stocker, S. N. Magonov, H. J. Cantow. Polym. Bull, 1991**;** 26: 209-214.
8. K, Okada, K, Watanabe, T. Urushihara, A. Toda, M. Hikosaka. Polymer, 2007; 48: 401-408.
9. Z. S. Zhang, C. G. Wang, Z.G. Yang, C. Y. Chen, K. C. Mai. Polymer, 2008; 49: 5137-5145.
10. Q. Xing, X. Q. Zhang, X. Dong, G. M. Liu, D. J. Wang. Polymer, 2012; 53: 2306-2314.
11. H. Tsuji, H. Takai, N. Fukuda, H. Takikawa. Macromol. Mater. Eng., 2006**;** 291: 325–335.
12. H. Tsuji, K. Tashiro, L. Bouapao, J. Narita. Macromol. Mater. Eng., 2008; 293: 947–951.
13. W. Zhou, B. Duan, M. Wang, W. Cheung. J. Appl. Polym. Sci., 2009; 113: 4100–4115.
14. Y. Zhao, Z. Qiu, W. Yang. J. Phys. Chem. B, 2008; 112: 16461–16468.
15. H.P. Pan, Z.B. Qiu. Macromolecules, 2010**;** 43: 1499–1506.
16. H, Bai, W. Zhang, H Deng, Q Zhang, Q Fu. Macromolecules, 2011**;** 44: 1233–1237.
17. H. Li, M. A. Huneault. Polymer, 2007**;** 48: 6855–6866.
18. Z. B. Qiu, Z. S. Li. Ind. Eng. Chem. Res., 2011**;** 50: 12299–12303.
19. H. Tsuji, H. Takai, S. Saha. Polymer, 2006; 47: 3826–3837.
20. Y. Li, C. Y. Han. Ind. Eng. Chem. Res., 2012**;** 51: 15927–15935.
21. T. Wen, Z. J. Xiong, M. Liu, X. Q. Zhang, D. V. Sicco, W. Ryan, A. P. Cornelis, Joziasse, F. Wang, D. Wang. Polymer, 2013; 54: 1923-1929.
22. Q. L. Dong, Y. Li, C. Y. Han, X. Zhang, K. Xu, H. L. Zhang, L. S. Dong. J. Appl. Polym. Sci., 2013; 130: 3919–3929.
23. S. Schmidt, M. Hillmyer. J. Polym. Sci. Pol. Phys., 2001; 39: 300-313.
24. P. J. Pan, Z. C. Liang, A. M. Cao, Y, Inoue. ACS Appl. Mater. Inter., 2009**;** 1: 402−411.
25. S. S. Wang, C. Y. Han, J. J. Bian, L. L. Han, X. M. Wang, L. S. Dong. Polym. Int., 2011; 60: 284−297.
26. L. J. Han, C. Y. Han, J. J. Bian, Y. J. Bian, H. J. Lin, X. M. Wang, H. L. Zhang, L. S. Dong. Polym. Eng. Sci ., 2012; 52: 1474-1484.
27. J. J. Hwang, S. M. Huang, H. J. Liu, H. C. Chu, L. H. Lin, C. S. Chung. J .Appl. Polym. Sci., 2012**;** 124: 2216-2226.
28. E. Picard, E. Espuche, R. Fulchiron. Appl. Clay. Sci., 2011; 53: 58-65.
29.V. Ojijo, S. S. Ray, R. Sadiku. Acc. Chem. Res., 2012; 4: 2395-2405.
30. S. S. Ray. Acc. Chem. Res., 2012; 45; 1710.
31. V. Krikorian, D. J. Pochan. Macromolecules, 2004**;** 37: 6480-6491.
32. H. L. Qin, S. M. Zhang, H. J. Liu , S. B. Xie, M. S. Yang, D. Y. Shen. Polymer, 2005; 46: 3149-3156.
33. G. Guerrero, P. H. Mutin , A. Vioux. Chem. Mater., 2001; 13: 4367-4373 .
34. X. Dai, Z. S. Zhang, C. G. Wang, Q. Ding, J. Jiang. K. Mai. Composites Part A, 2013; 49: 1-8.
35. X. Dai, Z. S. Zhang, C. G. Wang, Q. Ding, J. Jiang. K. Mai. Compos. Sci. Technol., 2013; 89**:** 38-43.
36. E. W. Fischer, H. J. Sterzel, G. Wegner. Kolloid-Z Polym., 1973; 251: 980–990.
37. A. Sodergard , M. Stolt. Prog. Polym. Sci., 2002; 27: 1123-1163.
38. M. Murariu, A. Doumbia, L. Bonnaud, A. L. Dechief, Y. Paint, M. Ferreira, et al, Biomacromolecules, 2011; 12: 1762-1771.
39. M. Avrami. J. Chem. Phys., 1939; 7: 1103-1112..
40. M. Avrami. J. Chem. Phys., 1940; 8: 212−224.
41. A. M. Harris, E. C. Lee. J. Appl. Polym. Sci., 2008; 107: 2246-2255.
42. K. A. Mauritz, E. Baer, A. J. Hopfinger. J. Polym. Sci. D Macromol Rev., 1978; 13: 1-61.
43. T. Kawai, R. Iijima, Y. Yamamoto, T. Kimura. Polymer, 2002; 43: 7301-7306.
44. H. G. Haubruge, R. Daussin, A. M. Jonas, R. Legras, J. C. Wittmann, B. Lotz. Macromolecules, 2003; 36: 4452-4456.
45. N. Jacquel, K. Tajima, N. Nakamura, H. Kawachi, P. J. Pan, Y. Inoue. J. Appl. Polym. Sci., 2010; 115: 709-715.
46. W. John, D. Mark, L. Hans-Conrad. J. Chem. Crystallogr., 2007; 37: 103-108.
47. W. Hoogsteen, A. Postema, A. Pennings, G. Brinke, P. Zugenmaier. Macromolecules, 1990; 23: 634–642.
48. Z. Q. Su, M. Dong, Z. X. Guo , J Yu. Macromolecules, 2007; 40: 4217-4224.
49. W.C. Lai, W.B. Liau, and T.T. Lin. Polymer, 2004**;** 45: 3073-3080.

Figure captions

Figure 1. (a)DSC heating curves of PPOA and PPOA supported on MMT with various MMT/PPOA mass ratio at a heating rate of 10 ^{o}C min^{-1}; (b) FTIR spectrum of M_0, M_5, PPOA and PPCa at room temperature.

Figure 2．The WAXD profiles of (a)M_0, M_5, $5PM_0$ and $5PM_5$ and (b)M_5.

Figure 3. DSC curves of (a) nonisothermal crystallization and (b) subsequent melting for pure PLLA, PLLA/talc2, PLLA/PPCa2, PLLA/MMT and PLLA/NMMT blends. Both the cooling and heating rates are 10 ^{o}C min^{-1}.

Figure 4. DSC curves of (a) nonisothermal crystallization and (b) subsequent melting for PLLA/NMMT blends with different M_5 contents. Both the cooling and heating rates are 10 ^{o}C min^{-1}.

Figure 5. DSC exotherms of isothermal crystallization at 140 ^{o}C for pure PLLA, PLLA/talc2, PLLA/PPCa2, PLLA/MMT and PLLA/NMMT blends.

Figure 6. (a) Conversion curves and (b) Avrami plots of pure PLLA, PLLA/talc2, PLLA/PPCa2, PLLA/MMT and PLLA/NMMT blends isothermally crystallized at 140 ^{o}C.

Figure 7. POM photographs of pure PLLA and its blends isothermally crystallized at 130 ^{o}C. (a)PLLA; (b)$5PM_0$; (c)PLLA/talc2; (d)PLLA/PPCa2; (e)$2.5PM_5$; (f)$5PM_5$; (g)$7.5PM_5$; (h) $10PM_5$.

Figure 8. Schematic diagrams of prepared PLLA/NMMT nanocomposites.

Figure 9. Typical stress versus strain curves of pure PLLA and PLLA/NMMT blends, (a) without annealing; (b) annealed at 130 ^{o}C for 2 min.

Figure 10. WAXD patterns of pure PLLA and PLLA/NMMT blends annealed at 130 ^{o}C for 2 min.

Figure 11.Temperature dependence of storage modulus for pure PLLA and PLLA/NMMT blends after heat treatment.

TOC
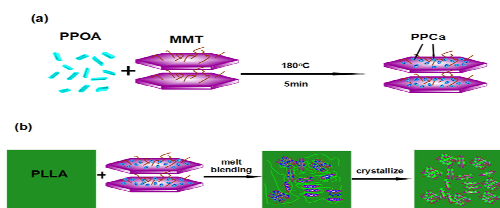
Crystallization of poly(L-lactide) could be greatly enhanced by a montmorillonitic substrate favoring nucleation.